Development 129, 361-372 (2002)
Printed in Great Britain © The Company of Biologists Limited 2002
DEV3528

Hedgehog is required for murine yolk sac angiogenesis

Noah Byrd[1], Sandy Becker[1], Peter Maye[1], Roopa Narasimhaiah[1], Benoit St-Jacques[2], Xiaoyan Zhang[3], Jill McMahon[3], Andrew McMahon[3] and Laura Grabel[1,*]

[1]Department of Biology, Wesleyan University, CT 06459, USA
[2]Genetics Unit, The Shriners Hospital for Children, Montreal, Quebec H3G 1A6, Canada
[3]Department of Molecular and Cellular Biology, The Biological Laboratories, Harvard University, Cambridge, MA 02138, USA
*Author for correspondence (e-mail: lgrabel@wesleyan.edu)

Accepted 19 October 2001

SUMMARY

Blood islands, the precursors of yolk sac blood vessels, contain primitive erythrocytes surrounded by a layer of endothelial cells. These structures differentiate from extra-embryonic mesodermal cells that underlie the visceral endoderm. Our previous studies have shown that Indian hedgehog (*Ihh*) is expressed in the visceral endoderm both in the visceral yolk sac in vivo and in embryonic stem (ES) cell-derived embryoid bodies. Differentiating embryoid bodies form blood islands, providing an in vitro model for studying vasculogenesis and hematopoiesis. A role for *Ihh* in yolk sac function is suggested by the observation that roughly 50% of *Ihh*$^{-/-}$ mice die at mid-gestation, potentially owing to vascular defects in the yolk sac. To address the nature of the possible vascular defects, we have examined the ability of ES cells deficient for *Ihh* or smoothened (*Smo*), which encodes a receptor component essential for all hedgehog signaling, to form blood islands in vitro. Embryoid bodies derived from these cell lines are unable to form blood islands, and express reduced levels of both PECAM1, an endothelial cell marker, and α-SMA, a vascular smooth muscle marker. RT-PCR analysis in the *Ihh*$^{-/-}$ lines shows a substantial decrease in the expression of *Flk1* and *Tal1*, markers for the hemangioblast, the precursor of both blood and endothelial cells, as well as *Flt1*, an angiogenesis marker. To extend these observations, we have examined the phenotypes of embryo yolk sacs deficient for *Ihh* or *Smo*. Whereas *Ihh*$^{-/-}$ yolk sacs can form blood vessels, the vessels are fewer in number and smaller, perhaps owing to their inability to undergo vascular remodeling. *Smo*$^{-/-}$ yolk sacs arrest at an earlier stage: the endothelial tubes are packed with hematopoietic cells, and fail to undergo even the limited vascular remodeling observed in the *Ihh*$^{-/-}$ yolk sacs. Our study supports a role for hedgehog signaling in yolk sac angiogenesis.

Key words: Hedgehog, Indian hedgehog, Angiogenesis, Vasculogenesis, Hematopoiesis, Embryoid bodies, Yolk sac, Mouse

INTRODUCTION

The first site of blood and blood vessel formation in the mouse is the extra-embryonic visceral yolk sac (Boucher and Pedersen, 1996; Palis et al., 1995). Yolk sac morphogenesis is based on complex tissue interactions during and after gastrulation, which are guided by a wide array of signaling molecules. The visceral yolk sac is composed of two cell layers, visceral endoderm and the underlying extra-embryonic mesodermal layer. Blood islands form around 7-7.5 dpc from localized mesodermal masses lying interior to the visceral endoderm (Palis et al., 1995). These masses contain hemangioblasts, the proposed common precursors of both primitive erythrocytes and endothelial cells (Choi et al., 1998; Robb and Elefanty, 1998). Endothelial cells then form an outer layer, surrounding a pocket containing loosely packed, differentiating red blood cells. Mesodermally derived mesothelial cells provide the outer most layer of the blood island, and line the visceral endoderm between blood islands.

Vasculogenesis, the in situ differentiation of mesoderm into endothelial cell-containing tubes, occurs shortly after the onset of blood island formation in the visceral yolk sac. The resulting endothelial tubes then form a three-dimensional network of tubules that constitutes the primary vascular plexus, which then undergoes reorganization, sprouting and remodeling through the process of angiogenesis to form the large vitelline vessels (Flamme et al., 1997; Risau, 1997; Risau and Flamme, 1995). This remodeling is accompanied by the recruitment and differentiation of vascular smooth muscle cells, derived most likely from the mesothelial layer. Hematopoiesis, the differentiation of primitive erythrocytes from mesodermal precursors (hemangioblasts), occurs concomitantly with vasculogenesis. Several genes are involved in the process of vasculogenesis and angiogenesis, including *Flk1* (*Kdr* – Mouse Genome Informatics) (Shalaby et al., 1995) *Flt1* (encoding vascular endothelial growth factor receptor 1) (Fong et al., 1995), *Cd34* (Cheng et al., 1996), *Vegf* (Carmeliet et al., 1996; Ferrara et al., 1996), and *Tie2* (*Tek* – Mouse Genome Informatics) (Sato et al., 1995). The importance of these genes in vascular morphogenesis has been well supported by phenotypic analysis of targeted mutations in mice.

Embryonic stem (ES) cell embryoid bodies can form blood

island-like structures in vitro and mimic many of the differentiation events that occur in the yolk sac. Pluripotential ES cells proliferate in an undifferentiated state and spontaneously differentiate into embryoid bodies when grown in suspension. Morphologically, embryoid bodies are characterized by an outer layer of extra-embryonic endoderm surrounding a core of cells analogous to the epiblast, the source of all three primary germ layers in the embryo. The embryoid body core then undergoes cavitation, using spatially localized programmed cell death, in a manner analogous to the formation of the amniotic cavity in the embryo (Coucouvanis and Martin, 1995; Coucouvanis and Martin, 1999). At later stages of development, embryoid body differentiation includes the formation of blood island structures containing blood cells and endothelial cells, providing a model to study the processes of vasculogenesis and hematopoiesis (Doetschman et al., 1985; Hirashima et al., 1999; Vittet et al., 1996).

Hedgehog signaling is essential for proper pattern formation and morphogenesis in several species (McMahon, 2000). There are three mouse homologs of the *Drosophila* hedgehog (*Hh*) gene: sonic hedgehog (*Shh*), desert hedgehog (*Dhh*) and Indian hedgehog (*Ihh*) (Echelard et al., 1993; Hammerschmidt et al., 1997). All three hedgehog genes in the mouse signal through a highly conserved signaling pathway that includes a receptor patched (Ptch), a twelve pass membrane-bound ligand binding component, and smoothened (Smo; Smoh – Mouse Genome Informatics), a seven pass G-protein-like molecule, that is responsible for transducing the Hh signal (Denef et al., 2000; Murone et al., 1999). Hedgehog-dependent transcriptional activation is mediated by three vertebrate homologs to the *Drosophila* Cubitus interruptus (Ci) transcription factor: Gli1, Gli2 and Gli3. Downstream target genes include *Ptch*, whose upregulation serves as an indicator of a hedgehog response, as well as bone morphogenic proteins (BMPs).

Ihh is expressed in the visceral endoderm of the yolk sac beginning at 6.5 dpc (Becker et al., 1997; Grabel et al., 1998) and the inner, mesodermal layer responds to hedgehog signaling by upregulating *Ptch* expression (Maye et al., 2000). The visceral endoderm has been proposed to be the source of inductive signals necessary for proper yolk sac vascular morphogenesis to occur (Dyer et al., 2001; Farrington et al., 1997; Palis et al., 1995). A recent study supports the hypothesis that Ihh secreted by the visceral endoderm cells promotes the differentiation of posterior epiblast cells into both endothelial and red blood cells (Dyer et al., 2001). Our previous studies using pharmacological inhibitors of Hh signaling in embryoid bodies have also suggested a role for Ihh in yolk sac differentiation (Maye et al., 2000). Consistent with these observations, 50% of Ihh-deficient embryos die at midgestation, perhaps owing to defects in the yolk sac. The other 50% die at birth, most likely because of respiratory failure as a result of a truncated rib cage – one example of the multiple defects in bone morphogenesis observed in the mutant (St-Jacques et al., 1999). A role for hedgehog signaling in blood vessel formation is supported by several observations. These include the hypervascularization of neurectoderm in response to overexpression of *Shh* (Rowitch et al., 1999), the decreased vascularization of lung tissue in *Shh*-deficient mice (Pepicelli et al., 1998) and the defective vascularization observed in the zebrafish *Shh* mutation (Brown et al., 2000).

To determine the role of hedgehog signaling in yolk sac vascular morphogenesis, we now examine the differentiation of *Ihh*- and *Smo*-deficient ES cell embryoid bodies and embryo yolk sacs. We find that the absence of hedgehog signaling leads to the inhibition of blood island differentiation in ES embryoid bodies and to defects in vascular remodeling in embryos.

MATERIALS AND METHODS

Generation of *Ihh* null ES cells

R1 ES cells (courtesy of Patricia Labosky) were electroporated with a linearized *Ihh* targeting construct designed to replace exon 1 with a neomycin resistant (neo^R) cassette. The construct (St-Jacques et al., 1999) was modified to include a point mutation in the neo^R cassette, making it less resistant to neomyocin (G418, Sigma). This modification facilitates the generation of homozygous transfectants using higher concentrations of G418 (Mortensen et al., 1992). The targeting construct also contains a thymidine kinase gene downstream of the neo^R cassette for selection against random insertion events. Heterozygous cell lines (clones 14 and 37) were recovered after culture of electroporated cells with 200 μl/ml G418 and 2×10^{-6} M gancyclovir (FIAU). Heterozygous cell lines were then cultured in the presence of 2 mg/ml G418, resulting in two $Ihh^{-/-}$ cell lines, clones 14-61 and 14-63I. The identification of null cell lines was confirmed by both PCR and Southern blot analyses. Primers to amplify the targeted construct were: 5′ neo, ATTCGCAGCGCATCGCCTTCTATCGCCTTC; 3′ Ihh, CAGCACCCGGTCTCCTGGCTTTACAGCTGA. PCR conditions were 5 minutes at 95°C, then 10 cycles of 30 seconds at 94°C, 1 minute at 60°C, 4 minutes 30 seconds at 72°C, then 35 cycles of 30 seconds at 94°C, 1 minute at 64°C and 4 minutes 30 seconds at 72°C. Primers to amplify the endogenous *Ihh* gene have been described previously (Maye et al., 2000). The conditions were 5 minutes at 95°C, then 35 cycles of 30 seconds at 94°C, 1 minute at 59°C, 3 minutes at 72°C, followed by 7 minutes at 72°C. The probe for the Southern blotting is taken from St-Jacques et al. (St-Jacques et al., 1999). The Southern hybridization was performed using Expressyb from Clontech and a digoxigenenin-labeled probe, and was visualized with CSPD (Roche).

Culture of ES cells

Both parental and transfected ES cell lines were maintained on STO or neo-resistant STO fibroblast feeder layers in DMEM (Gibco) and 15% fetal calf serum (Gibco) in the presence of recombinant LIF. Embryoid bodies were formed by removing the stem cells from the feeder layer and culturing them in suspension in medium without LIF (Doetschman et al., 1985). R1 ES cells heterozygous for insertion of a *lacZ* reporter gene at the *Ptch1* locus (courtesy of Matthew Scott) were grown and differentiated as described.

Breeding mice and genotyping mice and embryos

Mice containing a null allele of *Ihh* were previously generated (St-Jacques et al., 1999). Timed matings between heterozygous animals (identified by PCR as described by St-Jacques et al. (St-Jacques et al., 1999)) were set up to yield litters for harvest at 9.5, 10.5, 11.5 and 12.5 dpc. Part of each embryo was removed for PCR genotyping, using primers and conditions as described by St-Jacques et al. (St-Jacques et al., 1999).

In situ hybridization, immunocytochemistry and RT-PCR on embryoid bodies

Whole-mount in situ hybridization on embryoid bodies was performed as described by Maye et al. (Maye et al., 2000). Whole-mount immunocytochemistry was performed by blocking freshly fixed (not dehydrated) embryoid bodies all day in 3% powdered milk, 0.1% Triton X-100 in phosphate-buffered saline (PBS) at 4°C., incubating with primary antibody overnight on a rocker at 4°C,

followed by five 1 hour washes with blocking solution and incubation with secondary antibody overnight at 4°C. This was followed by five 1 hour washes in blocking solution, followed by a 20 minute incubation in PBS, 0.2% bovine serum albumin (BSA) and 0.1% TritonX-100. Color was developed using DAB (Sigma) plus 0.5% nickel chloride (NiCl). Primary antibodies used were as follows: PECAM1 (Mec13.3 from Pharmingen) 1/500; Flk1 (Vegf-R2, Ly-73 from Pharmingen) 1/50; αSMA (1A4 from Sigma) 1/500; and CD34 (RAM34 from Pharmingen) 1/50. A rabbit anti-rat HRP-conjugated secondary (Sigma) was used with PECAM, Flk1 and CD34 antibodies. A goat anti-mouse HRP conjugate (Transduction Laboratories) was used with αSMA antibodies. Photographs of intact embryoid bodies were taken before dehydrating, clearing and embedding in paraffin. RNA extraction, primers and conditions for RT-PCR were as described by Maye et al. (Maye et al., 2000). *Tal1* primers were as described by Robb et al. (Robb et al., 1995).

Immunostaining, in situ hybridization and histology on paraffin-embedded sections of embryos

After removal of part of each embryo for genotyping, each yolk sac and the remainder of the embryo was fixed, either in 3.7% formaldehyde overnight at 4°C or in a zinc fixative (0.05% calcium acetate, 0.5% zinc acetate, 0.5% zinc chloride in 1M Tris pH 7.4) overnight at room temperature. They were then dehydrated into 100% methanol, cleared in toluene, embedded in paraffin and sectioned. After dewaxing in xylene, sections were either stained with Hematoxylin and Eosin, or used for in situ hybridization or immunocytochemistry with the antibodies described above. In situ hybridization was as described by Wickramasinghe et al. (Wickramasinghe et al., 1995). The *Bh1* probe was a gift from James Palis. For immunocytochemistry, slides were incubated for 10 minutes in 1% H_2O_2 to quench endogenous peroxidases. After rinsing in PBS, they were blocked in PBS + 0.1% Triton X-100 + 5% appropriate serum for 30 minutes, followed by incubation overnight at 4°C in this blocking buffer containing primary antibody. After three washes in PBS, slides were incubated for 1-2 hours in blocking buffer containing secondary antibody. After three washes in PBS, the signal was visualized with DAB with or without 0.5% NiCl in PBS.

Whole-mount immunostaining on embryos

Whole-mount immunostaining was performed on 9.5, 10.5, 11.5 and 12.5 dpc yolk sacs as described at http://cbi.swmed.edu/ryburn/sato/htmprotocols/immunowholemount.htm. Color was developed as described above. Yolk sacs with embryos were then dehydrated and cleared in toluene before paraffin embedding and sectioning.

Photography and images

Slides were photographed using a Nikon E400 light microscope equipped with a Spot camera (Diagnostic Instruments), and processed using Adobe Photoshop. Whole embryos and embryoid bodies were photographed using an Olympus SZX12 dissecting microscope equipped with an Olympus DP11 digital camera.

RESULTS

Identification of hedgehog responding cells

In order to define the cell type(s) responding to the Ihh signal secreted by the visceral endoderm in ES embryoid bodies, we used an R1 ES cell line that is heterozygous for an insertion of a *lacZ* reporter gene at the *Ptch* locus (Goodrich et al., 1997). The insertion places the *lacZ* reporter gene under the control of the *Ptch* promoter. As *Ptch* is consistently a common downstream target of hedgehog signaling (McMahon, 2000) expression of β-galactosidase in these cells provides a measure of hedgehog response. Fig. 1A shows blood island morphology in R1 *Ptch-lacZ* embryoid bodies at day 13. *Ptch-lacZ* expression is localized in the mesodermal layer (mesothelial cells), adjacent to the source of Ihh signaling (visceral endoderm stained with eosin) and surrounding the blood islands (arrows, Fig. 1A). The position of the *Ptch*-expressing cells in a layer surrounding the blood island suggests that they could be endothelial, mesothelial or perhaps vascular smooth muscle cells. We therefore examined the expression of molecular markers for these cell types in both R1 *Ptch-lacZ* embryoid bodies and in the yolk sac mesodermal layer in *Ptch-lacZ* heterozygous mice. Platelet-endothelial cell adhesion molecule (PECAM) is an endothelial cell marker, and α smooth muscle actin (α-SMA) is a vascular smooth muscle cell and mesothelial cell marker (Hungerford and Little, 1999). Comparison of *Ptch-lacZ* expression with *Pecam* expression demonstrates that PECAM-positive cells lie interior to the zone of *Ptch-lacZ*-expressing cells (Fig. 1B). By contrast, α-SMA appears to overlap with regions of *Ptch-lacZ*-expressing cells in the outer most layer of blood islands and in the mesothelial cells that line the endoderm between blood islands (Fig. 1C). In day 10.5 dpc yolk sacs from *Ptch-lacZ* heterozygotes, β-galactosidase expression is also localized to the outermost layer surrounding blood vessels as well as to the mesothelial cells, between vessels (Fig. 1D). In these yolk sacs, α-SMA expression appears to localize to the same cell types that express β-galactosidase (Fig. 1E). Because upregulation of *Ptch* is an indicator of hedgehog signaling, these experiments suggest that mesothelial and perhaps vascular smooth muscle cells, but not endothelial cells, are the direct targets of the Ihh signal secreted by the visceral endoderm.

Generation of *Ihh*$^{-/-}$ ES cells and differentiation of *Ihh*$^{-/-}$ embryoid bodies

In order to examine the role of Ihh signaling in blood island differentiation, we generated *Ihh* deficient (*Ihh*$^{-/-}$) ES cell lines using a targeting construct (Fig. 2A) designed to replace exon 1 with a neomyocin resistance (neo^R) cassette that contains a point mutation in the neo^R open reading frame (Mortensen et al., 1992). This modification facilitates the generation of homozygous transfectants using higher concentrations of G418. Cell lines were generated as described in Materials and Methods. Identification of *Ihh* null cell lines was confirmed using PCR analysis (data not shown) and Southern analysis. Two *Ihh* heterozygous cell lines (clones 14 and 37, out of 96 screened) and two *Ihh* null cell lines (clones 14-61 and 14-63I, out of 144 screened) were obtained (Fig. 2B, and data not shown). The two heterozygous cell lines behaved identically in all assays, as did the two homozygous cell lines. Therefore, all studies shown use clone 14 as the heterozygous line and clone 14-61 as the homozygous cell line. As expected, the *Ihh*-null cell line did not express *Ihh* mRNA during embryoid body differentiation, based on RT-PCR analysis using a primer that recognizes a segment of the signaling peptide replaced by the (neo^R) cassette (Fig. 2C). Our previous data suggested that the upregulation of *Ptch* in embryoid body cores is a response to a hedgehog signal emanating from the visceral endoderm layer (Maye et al., 2000). This *Ptch* response is absent in the embryoid bodies derived from *Ihh*-deficient ES cells, confirming a role for Ihh signaling (Fig. 2D).

To determine if expression of *Shh* or *Dhh* is upregulated as

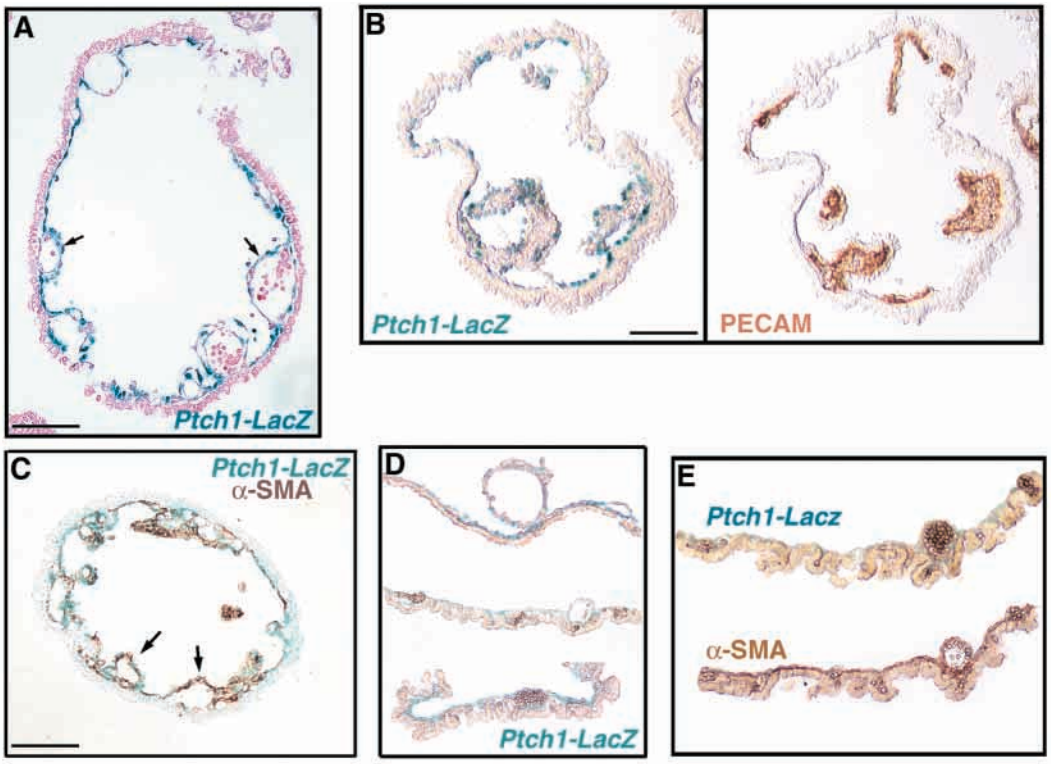

Fig. 1. Cell types responding to hedgehog signaling in ES embryoid bodies and yolk sacs. (A) Day 13 R1 ES *Ptch-lacZ* embryoid body expressing β-gal in the mesothelial layer surrounding blood islands (arrows) and beneath the visceral endoderm between blood islands. (B) *Ptch-lacZ* (β-gal) and PECAM are expressed in distinct patterns in adjacent sections in day 13 embryoid bodies. (C) Double staining demonstrates overlapping expression for β-gal and α-SMA around blood islands (arrows) and between them in day 12 embryoid bodies. (D) 10.5 dpc *Ptch-lacZ* yolk sacs express β-gal around blood vessels and in the mesothelial layer. (E) α-SMA is also expressed around and between vessels in 10.5 dpc yolk sacs. Scale bars: 100 μm.

a result of the absence of *Ihh* expression, we examined the expression of these genes using RT-PCR. Fig. 2C supports our previous report (Maye et al., 2000) and shows that *Shh* is expressed beginning at day 10 in embryoid bodies derived from $Ihh^{+/-}$ ES cells. The same pattern of upregulation is also observed in the mutant cell-derived embryoid bodies. *Dhh* is not expressed by either cell line during embryoid body differentiation (data not shown). These data suggest that the expression of *Shh* and *Dhh* are not altered by mutation of the *Ihh* gene.

If Ihh signaling plays a role in embryoid body differentiation, we would expect that the differentiation of *Ihh*-deficient cells would be compromised, in comparison with heterozygous cells. The first differentiation event visible in ES cell embryoid bodies is the appearance of an outer endodermal layer surrounding a core of epiblast-like cells (days 1-4). Most ES cell lines generate an outer layer of predominantly visceral endoderm, with some parietal endoderm. Embryoid bodies then begin to form a cavity, by spatially restricted programmed cell death reportedly regulated by BMP2 and BMP4 signaling (Coucouvanis and Martin, 1995) (days 4-7). As cavitation proceeds, the core cells beneath the visceral endoderm differentiate into a columnar epithelial layer analogous to embryonic ectoderm or epiblast, which eventually, as

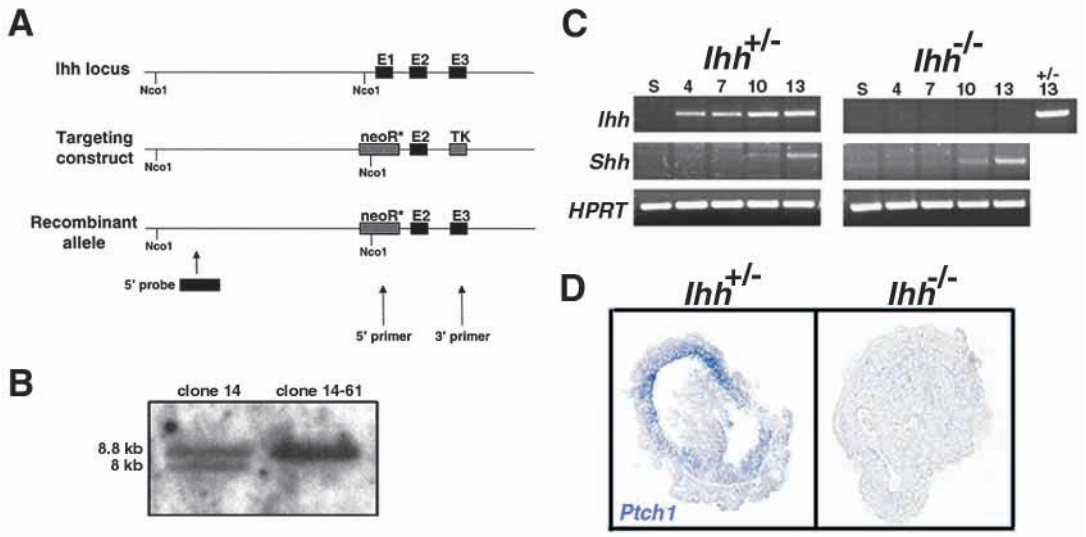

Fig. 2. Generation of *Ihh*-deficient ES cells. A targeting construct designed to replace the first exon with a neo^R cassette (A) was used to generate *Ihh* null cell lines (clone 14-61 and 14-63I (not shown)), identified using PCR (not shown) and Southern blot analysis (B). An *Nco*I digest yields an 8 kb endogenous allele and an 8.8 kb recombinant allele (see heterozygous clone14). Absence of *Ihh* mRNA expression and continued expression of *Shh* mRNA in *Ihh* null cell lines was demonstrated via RT-PCR analysis of embryoid body RNA (C) and loss of hedgehog response was detected by in situ hybridization analysis for *Ptch* in day 10 embryoid bodies (D).

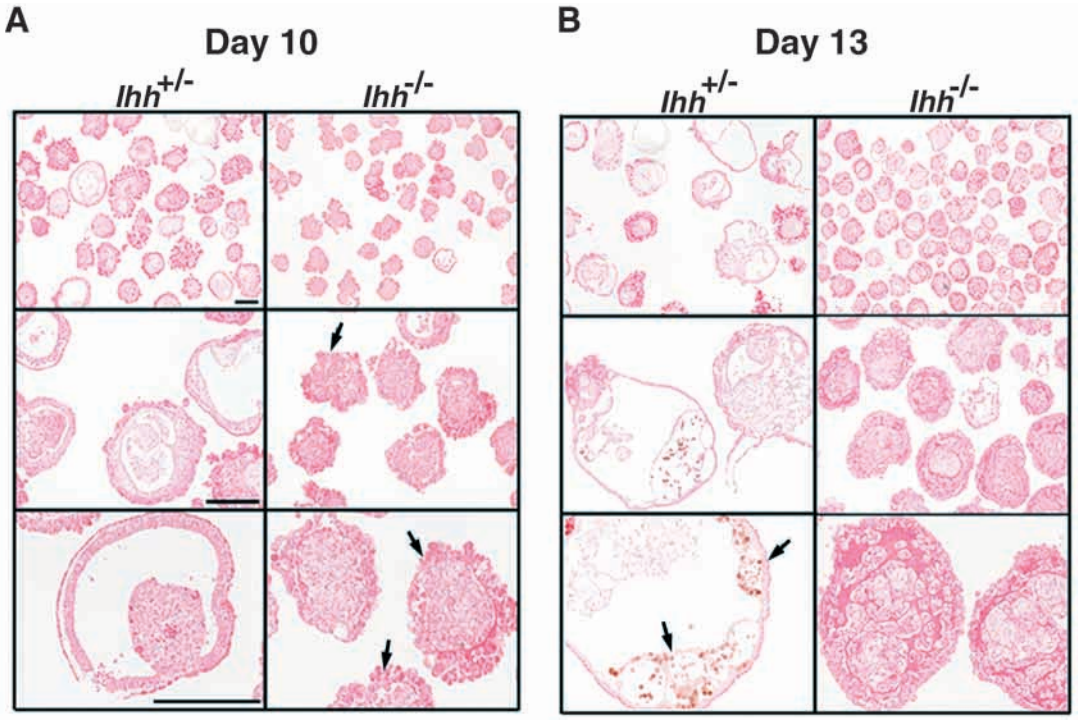

Fig. 3. Differentiation of *Ihh* deficient embryoid bodies. (A) Day 10 $Ihh^{-/-}$ embryoid bodies fail to cavitate compared with $Ihh^{+/-}$ embryoid bodies. $Ihh^{-/-}$ embryoid bodies also appear to have increased levels of parietal endoderm (arrows). (B) Day 13 $Ihh^{+/-}$ embryoid bodies contain blood cells (stained with benzidine) and blood islands (arrows), whereas $Ihh^{-/-}$ consistently fail to cavitate or form blood island structures. Scale bars: 100 μm.

in the embryo, gives rise to mesoderm and mesodermal derivatives (Vittet et al., 1996) (day 7 onwards). By day 7, *Ihh*-deficient embryoid bodies begin to appear smaller than embryoid bodies derived from heterozygous and wild-type lines (data not shown). On day 10, additional distinctions become apparent, with the $Ihh^{-/-}$ lines producing embryoid bodies that have largely failed to cavitate compared with the $Ihh^{+/-}$ lines (Fig. 3A). Cavitation in the mutant embryoid bodies is inhibited by 70% relative to the level observed for the embryoid bodies derived from heterozygous cells (note low power images in Fig. 3A,B). The decreased level of cavitation is accompanied by an apparent increase in extracellular matrix accumulation in the embryoid body interior. Mutant embryoid bodies also appear to have increased levels of a more rounded and loosely associated cell type in their outer layer than embryoid bodies derived from heterozygous cells (see arrows in Fig. 3). Parietal endoderm consists of rounded loosely associated cells that secrete high levels of extracellular matrix components, suggesting that $Ihh^{-/-}$ embryoid bodies have an increased proportion of parietal endoderm cells. We previously observed an analogous endoderm transition in embryoid bodies generated from wild-type ES cells that were treated with the hedgehog antagonist forskolin (Maye et al., 2000). Despite the apparent inhibition of cavitation observed in the embryoid bodies derived from *Ihh*-deficient cells, levels of *Bmp2* and *Bmp4* expression as assayed by RT-PCR, are unaltered relative to embryoid bodies derived from heterozygous cells (data not shown).

$Ihh^{-/-}$ embryoid bodies are deficient in their ability to form blood islands

By day 13 of development, the majority of wild-type (data not shown) and heterozygous embryoid bodies have matured to form blood islands containing erythrocytes that can be detected by benzidine staining (Fig. 3B). By contrast, *Ihh* deficient embryoid bodies appear unable to form blood islands (see Fig. 3B). The occasional cell-free pockets that form do not contain blood cells and do not appear to be surrounded by a layer of endothelial cells. To determine if endothelial cells were present in the mutant embryoid bodies despite the absence of apparent blood islands, we examined the expression of PECAM. By day 13, PECAM staining in $Ihh^{+/-}$ embryoid bodies is robust and present predominantly in the endothelial cells that line the inner layer of the blood island (arrows in Fig. 4). By contrast, the $Ihh^{-/-}$ embryoid bodies express PECAM at much lower levels and not in the cell layer surrounding the occasional cavity (arrowhead in Fig. 4A). Some diffuse staining is observed in the core region of both heterozygous and mutant embryoid bodies. (Fig. 4A, see Fig. 7). This core staining appeared to be localized to cells undergoing apoptosis, and we therefore used DAPI staining to determine if there were pyknotic nuclei, often observed in dying cells, in these regions. Pyknotic nuclei did coincide with regions of core PECAM staining for both mutant and heterozygous embryoid bodies, suggesting that this staining does not correspond to cells likely to contribute to blood island formation (data not shown). We also examined the expression of Flk1, a VEGF receptor important for vasculogenesis (Shalaby et al., 1995) and expressed by both hemangioblast and endothelial cells. Flk1 is expressed in $Ihh^{+/-}$ and $Ihh^{-/-}$ embryoid bodies in a pattern similar to that of PECAM (data not shown).

To further determine the extent of blood island differentiation in the mutant embryoid bodies, RT-PCR analysis was carried out to examine the expression of *Tal1*, a transcription factor necessary for blood formation (Elefanty et al., 1999; Visvader et al., 1998), *Flk1* and *Flt1*, an angiogenesis marker. *Tal1* and *Flk1* are expressed in the proposed hemangioblast, and thus their expression levels may reflect the relative abundance of this population of progenitors. Fig. 4B shows that in differentiating embryoid bodies at days 4-13, the levels of *Tal1*, *Flk1* and *Flt1* are sharply reduced in the absence of *Ihh*. These data suggest that in embryoid bodies Ihh is required for the formation of blood islands, including the differentiation of hemangioblast precursors and their yolk sac derivatives, endothelial cells and primitive erythrocytes.

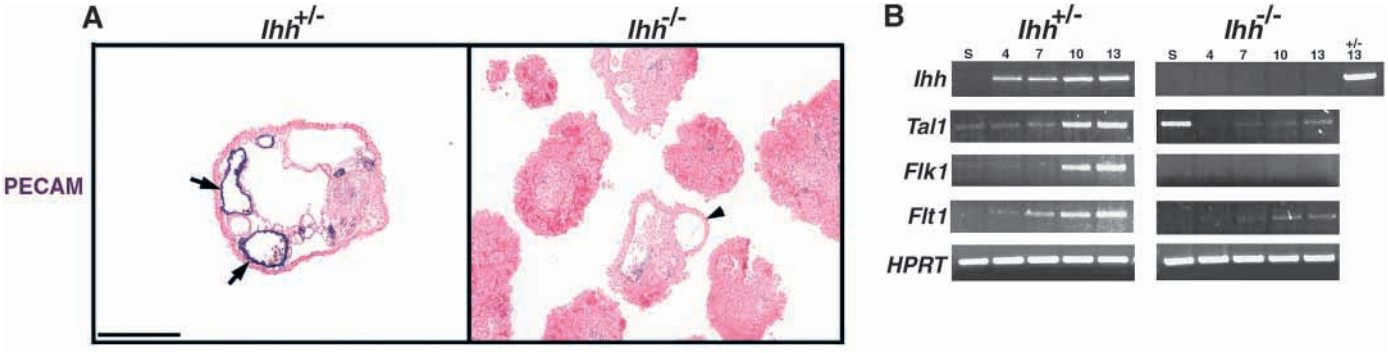

Fig. 4. Expression of vasculogenesis and hematopoiesis markers in *Ihh*$^{-/-}$ ES cell embryoid bodies. PECAM whole-mount immunocytochemistry in day 13 *Ihh*$^{+/-}$ embryoid bodies reveals expression in endothelial cells lining the interior of blood islands (A, arrows) and in core patches, whereas *Ihh*$^{-/-}$ embryoid bodies express PECAM in only core patches. Scale bar: 200 μm. (B) RT-PCR analysis examining expression of vasculogenesis and hematopoiesis markers. *Ihh*$^{+/-}$ embryoid bodies upregulate the markers *Tal1*, *Flk1* and *Flt1* during blood island development (days 10-13), whereas the loss of *Ihh* results in a dramatic reduction in mRNA levels for these genes. HPRT is shown as a loading control.

Ihh$^{-/-}$ yolk sacs exhibit abnormal vascular morphology

To complement our in vitro studies, we examined the phenotypes of *Ihh* heterozygous and *Ihh* mutant embryos and yolk sacs. It has been previously reported that roughly half of *Ihh*$^{-/-}$ embryos die between 10.5 and 12.5 days post coitum (dpc), possibly owing to yolk sac defects, the rest die just after birth (St-Jacques et al., 1999). At the end of the midgestation lethality period, at day 12.5, we therefore expect to observe only 12.5% mutant embryos in litters derived from heterozygous matings, whereas at earlier days we expect this percentage to be between 12.5 and 25%. This is consistent with our observation that 16% of the 200 9.5-13.5 dpc embryos examined were homozygous mutants. In whole-mount, 10.5 through 11.5 dpc *Ihh*$^{-/-}$ yolk sacs appeared less well vascularized than their heterozygous and wild-type littermates, suggesting a defect in yolk sac circulation (Fig. 5A). By day 10.5 dpc, wild-type and heterozygous yolk sacs are well into vascular remodeling, which produces large vitelline vessels, whereas the *Ihh*$^{-/-}$ yolk sacs appear deficient in this process and tend to have fewer, smaller, vessels (see Fig. 5A). This difference is pronounced by days 11.5 and 12.5 dpc, when heterozygous and wild-type yolk sacs appear to have completed vascular remodeling, resulting in an intricate orderly arrangement of large vitelline arteries and veins branching in a fractal pattern to smaller vessels. Day 11.5-12.5 dpc *Ihh*$^{-/-}$ yolk sacs clearly contain vessels, but they remain predominantly small and disorganized, suggesting an inability to complete remodeling (angiogenesis), which results in a compromised vascular network (see Fig. 5A, third row). Virtually all mutant embryos examined in whole mount appeared to have compromised vasculature, although the extent of the defect varied from subtle to more pronounced. Fig. 5B shows the pattern of PECAM staining in a whole heterozygous and mutant yolk sac, and supports the observation that the vessels formed in the absence of Ihh signaling are smaller and less well organized (Fig. 5, arrow) and can appear flattened (Fig. 5, arrowhead).

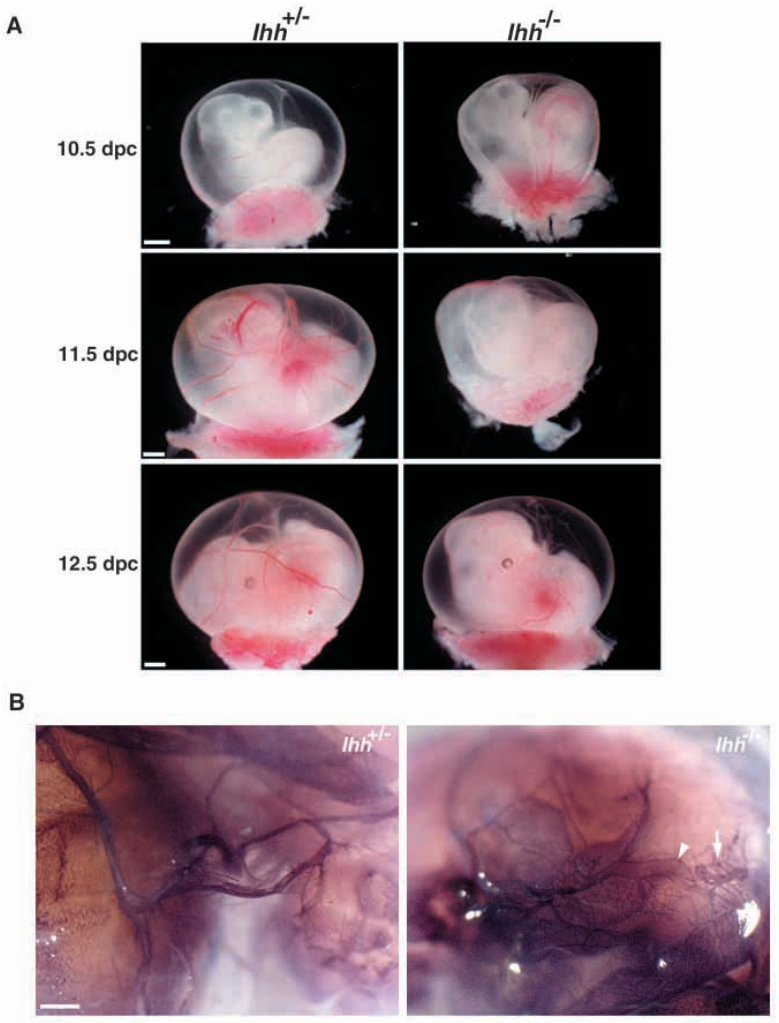

Fig. 5. Morphology of *Ihh*$^{-/-}$ yolk sacs. (A) 10.5, 11.5 and 12.5 dpc *Ihh* mutant yolk sacs display vascular defects. *Ihh*$^{-/-}$ yolk sacs contain fewer and smaller vessels and undergo suboptimal vascular remodeling compared with *Ihh*$^{+/-}$ yolk sacs. Scale bar: 1mm. (B) Whole-mount PECAM staining in 11.5 dpc yolk sacs. *Ihh*$^{+/-}$ vessels appear uniform in diameter and well organized. Note the small vessels (arrow) and flattened morphology (arrowhead) in the *Ihh*$^{-/-}$ yolk sac compared with the similar junction in the *Ihh*$^{+/-}$ yolk sac. Scale bar: 500 μm.

Histological analysis of 9.5 through 12.5 dpc yolk sac sections supports the conclusion that the vessels formed in the *Ihh* mutant yolk sacs are often smaller and/or flattened in their morphology (day 11.5 dpc embryo is shown in Fig. 6A). These defects are seen as early as 9.5 to 10.5 dpc and become more apparent by days 11.5 and 12.5 dpc, when the distal-most vessels in the mutants may appear flat (collapsed) and/or wider than normal (Fig. 6A).

Decreased levels of endothelial cell and vascular smooth muscle cell markers in mutant yolk sacs

To address the molecular nature of the vascular defects in *Ihh*$^{-/-}$yolk sacs, we examined the expression of PECAM, Flk1, α-SMA and CD34, an antigen expressed on the surface of hematopoietic precursors, as well as endothelial cells (Wood et al., 1997). At 9.5 dpc, PECAM is expressed robustly in the endothelial cell layer in *Ihh*$^{+/-}$ yolk sacs, but to a lesser extent in the mutants (data not shown). This distinction is maintained in both 10.5 and 11.5 dpc yolk sacs (Fig. 6B), and is also observed for Flk1 expression (Fig. 6B). We also examined CD34 expression in day 9.5 to 11.5 yolk sacs. We were able to detect weak expression of CD34 in the 9.5dpc *Ihh*$^{+/-}$ yolk sacs; however, none was detected in the *Ihh* $^{-/-}$ yolk sacs (data not shown). Stronger expression was detected in the heterozygous yolk sacs at 11.5 dpc, but expression was still absent in the mutant yolk sacs (Fig. 6B). Expression of CD34 was confined to endothelial cells and was never observed on round, hematopoietic-like cells in the heterozygous yolk sacs at the time points we observed.

At 9.5 dpc, α-SMA expression around the blood vessels is faint, in both *Ihh*$^{-/-}$ and *Ihh* $^{+/-}$ yolk sacs; however, by 10.5 dpc, expression levels around blood vessels increase in heterozygous yolk sacs but remain weak in the *Ihh* mutant yolk sacs (data not shown). By 11.5 dpc, expression of α-SMA is robust in the *Ihh*$^{+/-}$ yolk sacs and encircles the blood vessel whereas in the *Ihh*$^{-/-}$ yolk sacs, α-SMA expression appears predominantly restricted to the mesothelial layer (Fig. 6B). These results suggest that Ihh signaling may be necessary for the organization of endothelial cells and vascular smooth muscle cells in the yolk sac.

Smoothened$^{-/-}$ embryoid bodies resemble *Ihh*$^{-/-}$ embryoid bodies

The interpretation of data obtained from studies examining the role of hedgehog signaling using embryoid bodies deficient for *Ihh* is complicated by the possibility that other hedgehog genes may be expressed and therefore play roles in embryoid body differentiation. We have recently determined, using RT-PCR

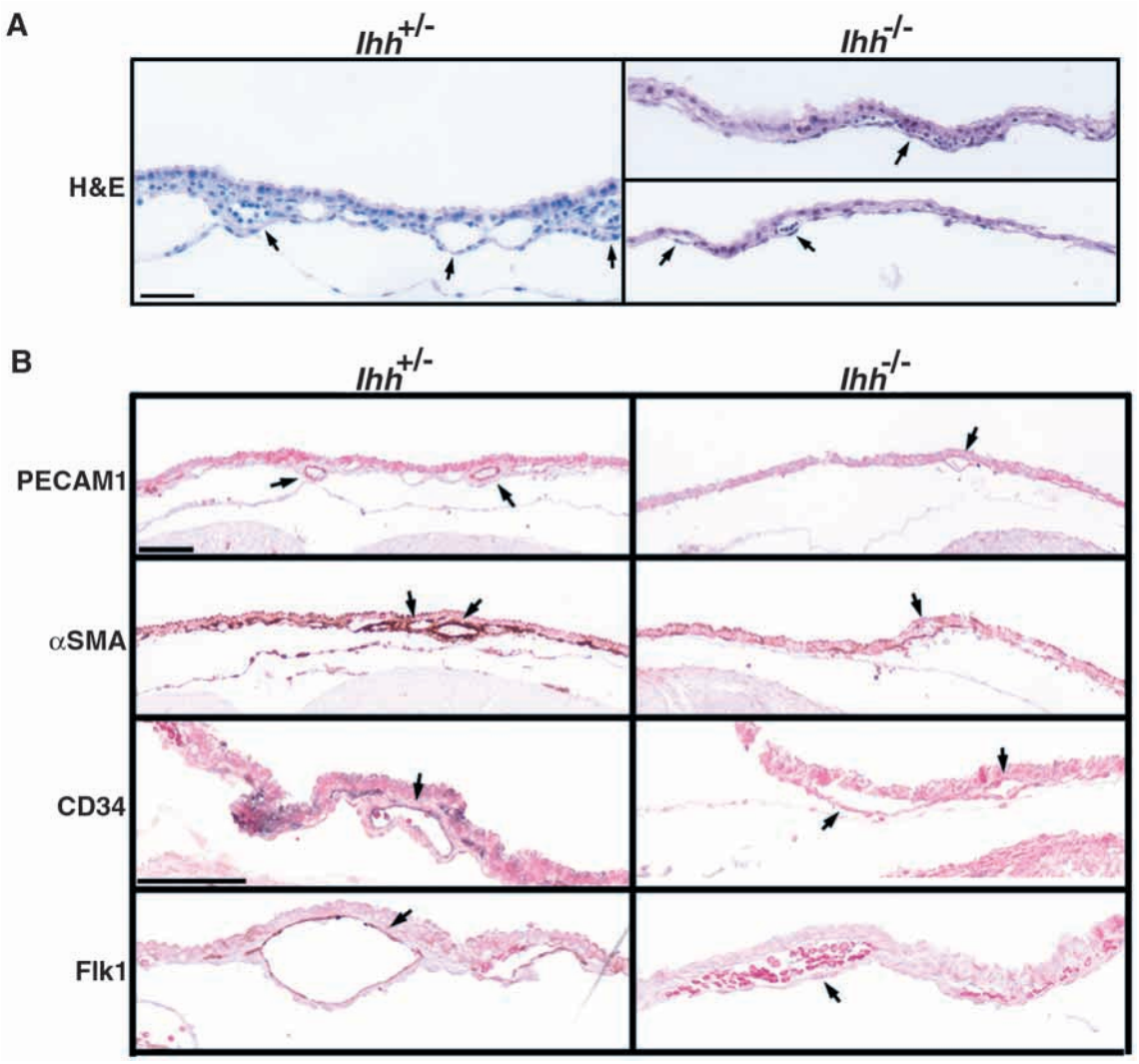

Fig. 6. Histological and immunocytochemical analysis of 11.5 dpc *Ihh*$^{+/-}$ and *Ihh* $^{-/-}$ yolk sacs. (A) Hematoxylin and Eosin stained sections illustrate the small diameter of blood vessels, as well as the flattened morphology, in mutant yolk sacs compared with heterozygotes (arrows). (B) PECAM stains endothelial cells more robustly in *Ihh* $^{+/-}$ yolk sacs than in *Ihh* mutants (first panel). α-SMA stains vascular smooth muscle cells encircling the blood vessels in *Ihh*$^{+/-}$ yolk sacs, whereas it fails to do so in the mutants (second panel, note arrow on right side). Additional endothelial cell markers, CD34 and Flk1, also exhibit reduced expression levels in the *Ihh* mutant yolk sacs compared with *Ihh*$^{+/-}$ yolk sacs (third and fourth panels). Scale bars: 100 μm.

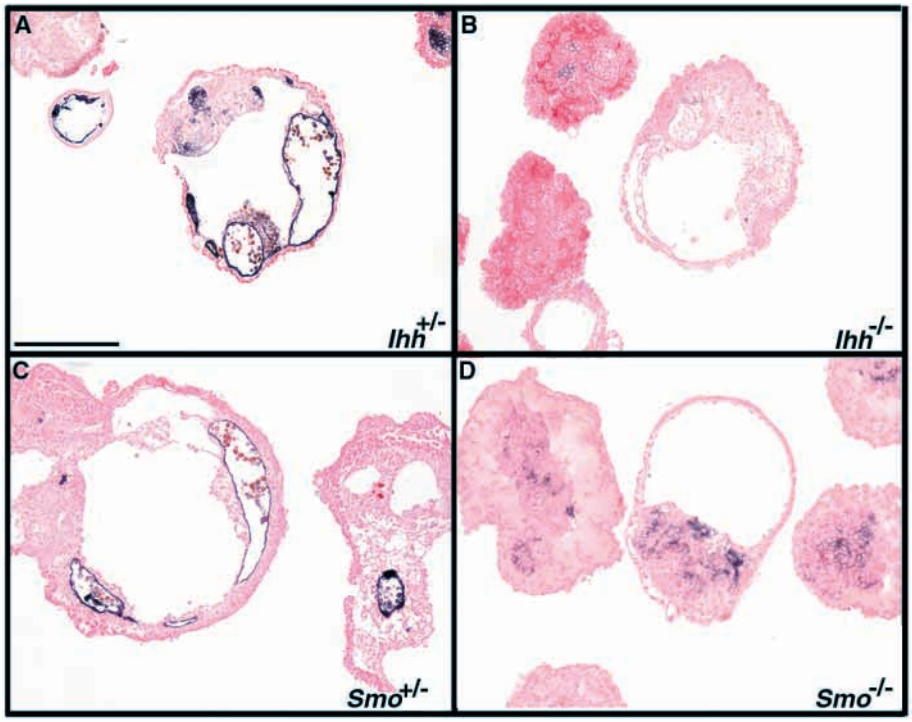

Fig. 7. *Smo*$^{-/-}$ embryoid bodies resemble *Ihh*$^{-/-}$ embryoid bodies. PECAM is expressed in endothelial cells lining the interior of the blood island and in core patches in day 13 *Ihh* and *Smo* heterozygous embryoid bodies (A,C). Like *Ihh*$^{-/-}$ embryoid bodies, the majority of *Smo*$^{-/-}$ embryoid bodies fail to cavitate and do not express PECAM in cell-free pockets, only in core patches (B,D). Scale bar: 200 μm.

analysis, that *Dhh* mRNA is not detectable in R1 ES embryoid body cultures (data not shown), but our previous studies, and data reported here (Fig. 2C), establish that *Shh* is expressed after day 11 in embryoid body core cells internal to the endoderm (Maye et al., 2000). To study the role of signaling mediated by all hedgehog genes, we examined the phenotype of *Smo*-deficient ES-cell derived embryoid bodies. *Smo* encodes the component of the Hh receptor complex thought to be required for all hedgehog signals, therefore, mutations in this gene effectively eliminate hedgehog signal transduction (Zhang et al., 2001). Derivation of the cell lines will be described elsewhere. The two heterozygous lines analyzed behaved identically to each other, as did the two homozygous cell lines. We therefore report the data obtained for one of the heterozygous lines and one of the homozygous lines.

Smo-deficient embryoid bodies have the same phenotype as the *Ihh*-deficient cell lines. In contrast to the heterozygous lines, which cavitate and form numerous blood islands, the vast majority of *Smo*-deficient embryoid bodies fail to cavitate (cavitation is inhibited by 78% compared with heterozygotes) and fail to form blood islands (Fig. 7). Again, *Bmp2* and *Bmp4* expression levels, based on RT-PCR analysis, are unaffected by the absence of hedgehog signaling in mutant embryoid bodies (data not shown). *Smo*$^{+/-}$ embryoid bodies, like *Ihh* heterozygotes, express robust levels of PECAM in blood island endothelial cells, whereas PECAM staining in *Smo* null lines does not localize to rare cell-free pockets, and is only found diffusely in core cells (Fig. 7), as in *Ihh*$^{+/-}$ embryoid bodies described above.

Smo$^{-/-}$ yolk sacs contain dense clusters of hematopoietic cells and fail to undergo angiogenesis

Smo$^{-/-}$ embryos die before turning (~9.5 dpc) (Zhang et al., 2001) and, as described below, display a more severe yolk sac phenotype than *Ihh*$^{-/-}$ embryos. To determine the extent of endothelial cell differentiation in *Smo*$^{-/-}$ yolk sacs, we analyzed PECAM expression. Whole-mount examination at 9.5 dpc clearly demonstrates that both *Smo*$^{+/-}$ and *Smo*$^{+/+}$ yolk sacs form robust vasculature, whereas *Smo*$^{-/-}$ yolk sacs fail to undergo angiogenesis and remain arrested in the primary vascular plexus stage (Fig. 8A). In the mutant yolk sac shown, the chicken-wire-like pattern of PECAM staining that characterizes the vascular plexus is restricted to the region most proximal to the placenta and does not extend around the circumference of the yolk sac. Analysis of sectioned yolk sacs reveals a blood cell phenotype not observed in the *Ihh*$^{-/-}$ yolk sacs. The tubules of endothelial cells formed in the mutant often contain dense clusters of hematopoietic cells, tightly packed within the tubule (Fig. 8B). This packed phenotype is most frequently observed proximal to the placenta. In situ hybridization analysis for expression of the embryonic globin gene *Bh1* (Wilkinson et al., 1987) confirms the identification of these cells as primitive erythrocytes (Fig. 8C). We examined PECAM expression in sections to observe more closely the extent of endothelial cell differentiation. The staining for PECAM was strong in *Smo*$^{+/-}$ or *Smo*$^{+/+}$ yolk sacs, highlighting blood islands and blood vessels, and significantly weaker in *Smo*$^{-/-}$ yolk sacs (Fig. 8D). These data suggest that the complete absence of hedgehog signaling leads to an inhibition of vascular remodeling, but that differentiation of primitive erythrocytes and some endothelial cells does proceed.

DISCUSSION

Previous studies have demonstrated the importance of the visceral endoderm layer in yolk sac vasculogenesis (Farrington et al., 1997; Palis et al., 1995) and identified Ihh as a key signal for this process (Dyer et al., 2001; Maye et al., 2000). A recent study using isolated epiblast tissue supports the hypothesis that Ihh secreted by the visceral endoderm cells promotes the differentiation of posterior epiblast cells into blood islands containing endothelial and red blood cells (Dyer et al., 2001). We now demonstrate using a gene targeting approach that hedgehog signaling is essential for normal yolk sac angiogenesis.

Hedgehog expression in the murine yolk sac

Hedgehog signaling molecules play numerous inductive and

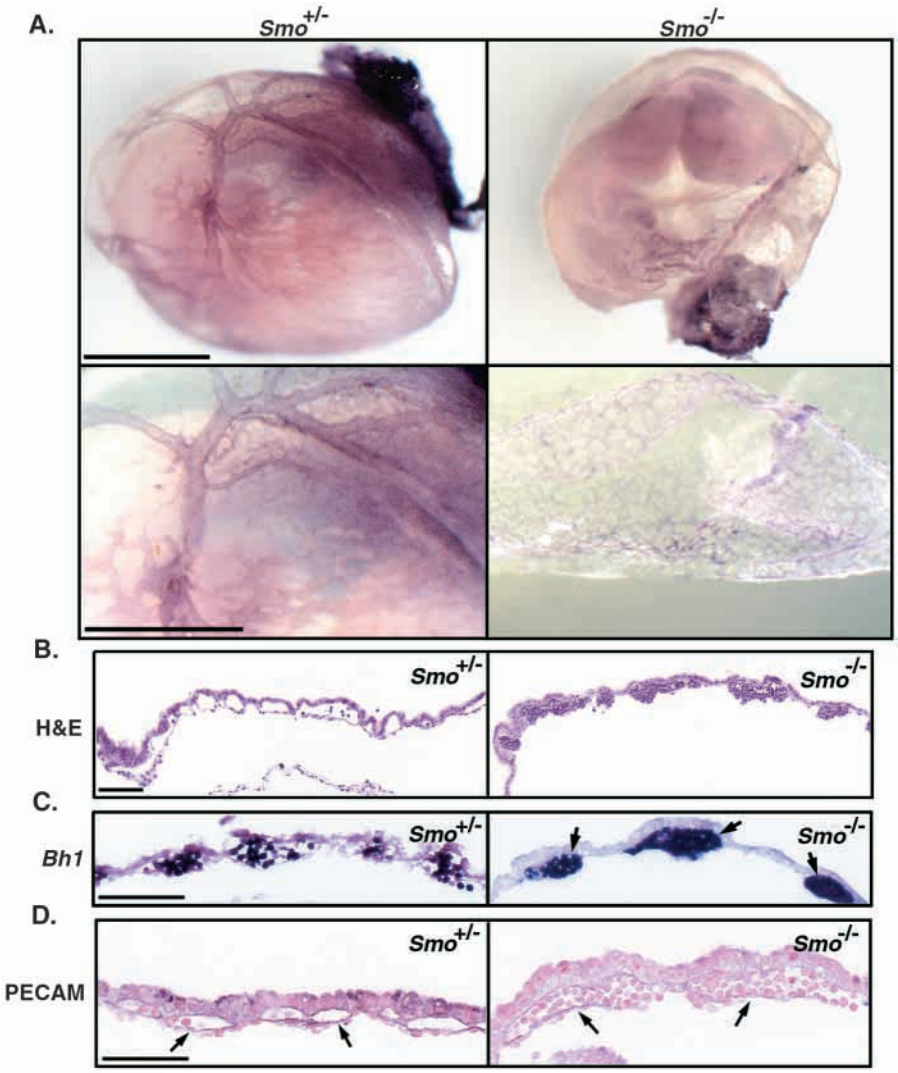

Fig. 8. *Smo* mutant yolk sacs exhibit severe vascular defects. (A) Whole-mount immunocytochemistry for PECAM demonstrates the arrest in the primary vascular plexus stage and total absence of large vitelline vessels in the mutant yolk sacs (note proximal staining in upper right panel and enlargements below). Scale bars: 1mm. (B) Hematoxylin and Eosin stained sections show the vessels packed with hematopoietic cells in the mutant yolk sacs compared with the heterozygotes. In situ hybridization for *Bh1* (C) identifies the clustered cells as erythrocytes. (D) PECAM staining is reduced in the *Smo* mutant yolk sacs compared with $Smo^{+/-}$ yolk sacs. Scale bars: 100 μm in B-D.

patterning roles in vertebrate and invertebrate development. In the mouse, the three hedgehog genes, *Shh*, *Ihh* and *Dhh*, have distinct and overlapping functions. In the yolk sac, there is no evidence for expression of *Shh*, whereas *Ihh* and *Dhh* have specific spatio-temporal expression patterns (Becker et al., 1997; Dyer et al., 2001; Farrington et al., 1997; Maye et al., 2000). *Ihh* is expressed in the visceral endoderm of the yolk sac beginning shortly after gastrulation (~6.5 dpc) and persisting after 12.5 dpc (Becker et al., 1997; Farrington et al., 1997; Maye et al., 2000). The mesodermal layer responds to hedgehog signaling by upregulating *Ptch* expression. Others have shown that *Dhh* is present in the yolk sac mesoderm, and to a lesser degree in the endoderm, from 10.5 dpc to 12.5 dpc (Farrington et al., 1997). These expression patterns coincide temporally with the formation of blood islands and the development of the yolk sac vasculature.

Loss of hedgehog signaling leads to blood island defects in ES embryoid bodies

Using a gene targeting approach, we generated $Ihh^{-/-}$ ES cells and examined their ability, in comparison with $Ihh^{+/-}$ ES cells, to differentiate as embryoid bodies. We show that loss of Ihh signaling from the visceral endoderm results in an overall decrease in the ability of embryoid bodies to cavitate compared with heterozygous lines. *Ihh*-deficient embryoid bodies are also severely compromised in their ability to form blood islands and produce primitive erythrocytes. The absence of blood islands may be attributable to the absence of ectoderm cells capable of generating the appropriate mesodermal precursors. Targeted mutagenesis of other genes has been shown to alter blood island differentiation in ES embryoid bodies. VE-cadherin- (a transmembrane protein necessary for endothelial cell-cell interactions) and VEGF-deficient ES cells produce embryoid bodies that contain endothelial and blood cells, but are unable to form a mature endothelial-cell derived vascular network (Ferrara et al., 1996; Vittet et al., 1997).

Ihh is not the only hedgehog gene expressed during embryoid body differentiation. We have shown that although *Dhh* is not detectable in embryoid bodies, *Shh* message accumulates in the embryoid body core at about 11 days (Maye et al., 2000). This pattern of *Shh* expression is also observed in the *Ihh*-deficient embryoid bodies (Fig. 2C), indicating these cells have hedgehog signaling activity caused by to *Shh*. Our observation that the phenotype of $Smo^{-/-}$ ES cell-derived embryoid bodies is virtually identical to $Ihh^{-/-}$ embryoid bodies suggests that *Shh* signaling does not contribute significantly to ES embryoid body cavitation or their differentiation into blood islands, perhaps owing to its delayed time of accumulation relative to *Ihh*. These results indicate the importance of Ihh signaling in ES cell embryoid body blood island development; no hematopoiesis or vasculogenesis can be detected in the absence of functional Ihh.

Loss of hedgehog signaling leads to angiogenesis defects of varying degrees in $Ihh^{-/-}$ and $Smo^{-/-}$ yolk sacs

It has been previously suggested that the mid-gestational lethality observed in $Ihh^{-/-}$ mice was attributable to defects in yolk sac morphogenesis (St-Jacques et al., 1999). We now present evidence in support of this hypothesis. Although it

appears that *Ihh*$^{-/-}$ yolk sacs can initiate vasculogenesis and hematopoiesis, they are deficient in their ability to undergo vascular remodeling. Mutant yolk sacs, at 10.5 to 11.5 dpc, are paler than those of heterozygous and wild-type littermates, most probably owing to reduced circulation of erythrocytes in mutants. Blood vessels are present, but they appear smaller and less organized than in the heterozygous yolk sacs. In addition, many of the blood vessels in mutant yolk sacs have a flattened morphology. Similar defects in yolk sac vascularization have also been observed in connexin 45-deficient mice (Kruger et al., 2000) and in yolk sacs deficient in endoglin, a TGF-β binding protein (Arthur et al., 2000; Li et al., 1999).

As defects in vascular morphogenesis could potentially be due to endothelial cell defects and/or vascular smooth muscle cell defects, we examined PECAM and α-SMA staining patterns. We have consistently observed reduced levels of PECAM staining in *Ihh*$^{-/-}$ yolk sacs compared with heterozygous and wild-type littermates. This observation is consistent with fewer endothelial cells being present, owing either to limited proliferation or differentiation. Several studies suggest that Shh can act as a mitogen (Britto et al., 2000), and evidence suggests that Ihh plays this role for chondrocytes (Karp et al., 2000). Reduced numbers of endothelial cells may contribute to the observed decrease in the number and diameter of blood vessels, as well as affect endothelial-dependent recruitment of mesenchymal cells to form the vascular smooth muscle cell layer. Reminiscent of the phenotype in endoglin-deficient yolk sacs in which vascular smooth muscle cells fail to encompass blood vessels (Li et al., 1999), we see a decrease in α-SMA staining around blood vessels in *Ihh*$^{-/-}$ yolk sacs. The loss of vascular integrity may also explain the collapsed vessels we see upon histological analysis of *Ihh*$^{-/-}$ yolk sacs. This type of defect may be attributed to an abnormal vascular smooth muscle cell layer, which can lead to a loss of vascular stability (Folkman and D'Amore, 1996). Flattened vessels may also result from a state of vascular regression caused by poor circulation in the yolk sac (Risau, 1997) and/or defects in the differentiation or recruitment of vascular smooth muscle cells (Darland and D'Amore, 1999). Previous studies support a role for hedgehog signaling in smooth muscle differentiation. In *Shh*-deficient lungs, the smooth muscle layer around the bronchi is absent (Pepicelli et al., 1998) and in *Ihh/Shh* double mutants, there is a reduced smooth muscle layer in the gut (Ramalho-Santos et al., 2000).

While this phenotypic analysis can explain the midgestation lethality of 50% of the *Ihh*$^{-/-}$ mutant embryos, why do the other 50% survive until birth? Mutations in other genes that result in abnormal yolk sac morphogenesis, such as the gene encoding factor V (Cui et al., 1996) and the gene encoding the tissue factor pathway inhibitor (Huang et al., 1997), also display midgestation lethality affecting only around 50% of the embryos. This observation may reflect the fading importance of the yolk sac after day 10 or so, when the placenta takes over its functions (Cross et al., 1994). If suboptimal vascularization has been sufficient to support development through this early period, the embryos will survive, despite compromised yolk sac function. In the case of the *Ihh*-deficient embryos, *Dhh* expression during 10.5 to 12.5 dpc, may provide the necessary cues to promote yolk sac morphogenesis through this critical period, at least in some of the embryos (Dyer et al., 2001). Given the observation that *Dhh* is expressed in the yolk sac, it was of interest to examine the yolk sac phenotype of *Smo*-deficient embryos. If *Dhh* plays a role in yolk sac morphogenesis, we would expect *Smo*$^{-/-}$ yolk sacs, which lack response to all hedgehog proteins, to arrest earlier and exhibit a more severe phenotype than *Ihh*$^{-/-}$ yolk sacs. Based upon PECAM staining of day 9 yolk sacs, the developing vasculature is arrested in the primary vascular plexus stage, blood vessels do not form and angiogenesis fails to occur.

Histological analysis of *Smo*$^{-/-}$ yolk sacs shows that the existing endothelial tubes are tightly packed with a large number of *Bh1*-expressing hematopoietic cells. The presence of excess blood cells may be attributable to a decrease in endothelial cell proliferation or differentiation, permitting more hemangioblast precursors to choose the hematopoietic pathway. Alternatively, the build up of erythrocytes may be a physical one, owing to the absence of a vasculature that can promote circulation. The decreased levels of PECAM staining observed in the mutant yolk sacs suggests that endothelial cell differentiation is compromised. Similar to *Ihh*$^{-/-}$ yolk sacs, *Smo*$^{-/-}$ yolk sacs exhibit reduced levels of α-SMA, consistent with a defect in the vascular smooth muscle cell layer. It has been demonstrated that signaling between the endothelial cell layer and the mesenchymal cells is essential for vascular stability and remodeling to occur properly, and that defects in one cell type may affect the function of the other (Conway et al., 2001; Folkman and D'Amore, 1996; Hirschi et al., 1998).

Comparison of embryoid bodies and embryo phenotypes

The differentiating yolk sac in vivo can be influenced by a number of cell types not present in the ES embryoid body system, including maternal tissue and extra-embryonic ectoderm. ES cell embryoid bodies deficient for *Ihh* or *Smo* exhibit more severe phenotypes than do *Ihh*$^{-/-}$ or *Smo*$^{-/-}$ yolk sacs. The mutant embryoid bodies are unable to generate endothelial or blood cells or to form blood islands, whereas the *Ihh*$^{-/-}$ and *Smo*$^{-/-}$ yolk sacs contain endothelial cells and erythrocytes and can form endothelial cell tubes and, in the case of *Ihh* mutants, undergo suboptimal remodeling. One possibility is that the ability of the *Ihh*$^{-/-}$ mutant yolk sacs to progress further than the *Smo*$^{-/-}$ yolk sacs is due to the presence of Dhh activity. It has previously been demonstrated that *Dhh* is expressed in the yolk sac beginning at day 10. There is no *Dhh* expressed, however, in ES embryoid body cultures, which may explain why both *Ihh*- and *Smo*-deficient cell lines apparently have identical defects. The observation that the complete absence of hedgehog signaling in *Smo*$^{-/-}$ ES cell embryoid body culture generates a more severe phenotype than the complete absence of hedgehog signaling in the embryo (no endothelial or blood cells differentiate in vitro) suggests that additional signals are present in vivo that are not produced in culture. These signals could be maternal or embryonic in origin and appear to be essential for initiating hematopoiesis and vasculogenesis. The *Smo*-deficient ES cells provide a useful model for identifying these signals.

We conclude that hedgehog signaling promotes the differentiation of endothelial cells and their remodeling to form blood vessels, but that the initial stages of differentiation can take place in the absence of this signal. Additionally, proper recruitment or differentiation of vascular smooth muscle cells is dependent on hedgehog signaling. Our observation that

primitive erythrocytes are present in *Smo*$^{-/-}$ yolk sacs suggests that this cell type is able to differentiate in the absence of hedgehog signaling, despite evidence that these cells can be induced by the addition of hedgehog peptides to epiblast cultures (Dyer et al., 2001). In fact, these blood cells may differentiate from the hemangioblast precursor at the expense of endothelial cells in the absence of hedgehog signal. A role for hedgehog signaling in angiogenesis is supported by the recent observation that Shh promotes angiogenesis by inducing angiogenic cytokines, including the VEGFs and angiopoietins (Pola et al., 2001). Our observation that *Ihh*$^{-/-}$ embryoid bodies are unable to upregulate the VEGF receptors *Flk1* and *Flt1* suggests that hedgehog signaling may be essential for upregulating the receptors for the VEGF cytokines as well. These observations suggest that hedgehog peptides may be useful therapeutic agents for promoting blood vessel sprouting.

We thank Ann C. Burke, Stephen Devoto and Michael Weir for critical reading of the manuscript and valuable suggestions; Patricia Labosky for R1 ES cells; Matthew Scott for *Ptch1-lacZ* ES cells; and James Palis for the BH-1 in situ probe. This work was supported by NSF grant IBN 9604367 and American Heart Association grant 0150284N to L. G.

REFERENCES

Arthur, H. M., Ure, J., Smith, A. J., Renforth, G., Wilson, D. I., Torsney, E., Charlton, R., Parums, D. V., Jowett, T., Marchuk, D. A. et al. (2000). Endoglin, an ancillary TGFbeta receptor, is required for extraembryonic angiogenesis and plays a key role in heart development. *Dev. Biol.* **217**, 42-53.

Becker, S., Wang, Z. J., Massey, H., Arauz, A., Labosky, P., Hammerschmidt, M., St-Jacques, B., Bumcrot, D., McMahon, A. and Grabel, L. (1997). A role for Indian hedgehog in extraembryonic endoderm differentiation in F9 cells and the early mouse embryo. *Dev. Biol.* **187**, 298-310.

Boucher, D. M. and Pedersen, R. A. (1996). Induction and differentiation of extra-embryonic mesoderm in the mouse. *Reprod. Fertil. Dev.* **8**, 765-777.

Britto, J. M., Tannahill, D. and Keynes, R. J. (2000). Life, death and Sonic hedgehog. *BioEssays* **22**, 499-502.

Brown, L. A., Rodaway, A. R., Schilling, T. F., Jowett, T., Ingham, P. W., Patient, R. K. and Sharrocks, A. D. (2000). Insights into early vasculogenesis revealed by expression of the ETS- domain transcription factor Fli-1 in wild-type and mutant zebrafish embryos. *Mech. Dev.* **90**, 237-252.

Carmeliet, P., Ferreira, V., Breier, G., Pollefeyt, S., Kieckens, L., Gertsenstein, M., Fahrig, M., Vandenhoeck, A., Harpal, K., Eberhardt, C. et al. (1996). Abnormal blood vessel development and lethality in embryos lacking a single VEGF allele. *Nature* **380**, 435-439.

Cheng, J., Baumhueter, S., Cacalano, G., Carver-Moore, K., Thibodeaux, H., Thomas, R., Broxmeyer, H. E., Cooper, S., Hague, N., Moore, M. et al. (1996). Hematopoietic defects in mice lacking the sialomucin CD34. *Blood* **87**, 479-490.

Choi, K., Kennedy, M., Kazarov, A., Papadimitriou, J. C. and Keller, G. (1998). A common precursor for hematopoietic and endothelial cells. *Development* **125**, 725-732.

Conway, E. M., Collen, D. and Carmeliet, P. (2001). Molecular mechanisms of blood vessel growth. *Cardiovasc. Res.* **49**, 507-521.

Coucouvanis, E. and Martin, G. R. (1995). Signals for death and survival: a two-step mechanism for cavitation in the vertebrate embryo. *Cell* **83**, 279-287.

Coucouvanis, E. and Martin, G. R. (1999). BMP signaling plays a role in visceral endoderm differentiation and cavitation in the early mouse embryo. *Development* **126**, 535-546.

Cross, J. C., Werb, Z. and Fisher, S. J. (1994). Implantation and the placenta: key pieces of the development puzzle. *Science* **266**, 1508-1518.

Cui, J., O'Shea, K. S., Purkayastha, A., Saunders, T. L. and Ginsburg, D. (1996). Fatal haemorrhage and incomplete block to embryogenesis in mice lacking coagulation factor V. *Nature* **384**, 66-68.

Darland, D. C. and D'Amore, P. A. (1999). Blood vessel maturation: vascular development comes of age. *J. Clin. Invest.* **103**, 157-158.

Denef, N., Neubuser, D., Perez, L. and Cohen, S. M. (2000). Hedgehog induces opposite changes in turnover and subcellular localization of patched and smoothened. *Cell* **102**, 521-531.

Doetschman, T. C., Eistetter, H., Katz, M., Schmidt, W. and Kemler, R. (1985). The in vitro development of blastocyst-derived embryonic stem cell lines: formation of visceral yolk sac, blood islands and myocardium. *J. Embryol. Exp. Morphol.* **87**, 27-45.

Dyer, M. A., Farrington, S. M., Mohn, D., Munday, J. R. and Baron, M. H. (2001). Indian hedgehog activates hematopoiesis and vasculogenesis and can respecify prospective neurectodermal cell fate in the mouse embryo. *Development* **128**, 1717-1730.

Echelard, Y., Epstein, D. J., St-Jacques, B., Shen, L., Mohler, J., McMahon, J. A. and McMahon, A. P. (1993). Sonic hedgehog, a member of a family of putative signaling molecules, is implicated in the regulation of CNS polarity. *Cell* **75**, 1417-1430.

Elefanty, A. G., Begley, C. G., Hartley, L., Papaevangeliou, B. and Robb, L. (1999). SCL expression in the mouse embryo detected with a targeted lacZ reporter gene demonstrates its localization to hematopoietic, vascular, and neural tissues. *Blood* **94**, 3754-3763.

Farrington, S. M., Belaoussoff, M. and Baron, M. H. (1997). Winged-helix, Hedgehog and Bmp genes are differentially expressed in distinct cell layers of the murine yolk sac. *Mech. Dev.* **62**, 197-211.

Ferrara, N., Carver-Moore, K., Chen, H., Dowd, M., Lu, L., O'Shea, K. S., Powell-Braxton, L., Hillan, K. J. and Moore, M. W. (1996). Heterozygous embryonic lethality induced by targeted inactivation of the VEGF gene. *Nature* **380**, 439-442.

Flamme, I., Frolich, T. and Risau, W. (1997). Molecular mechanisms of vasculogenesis and embryonic angiogenesis. *J. Cell Physiol.* **173**, 206-210.

Folkman, J. and D'Amore, P. A. (1996). Blood vessel formation: what is its molecular basis? *Cell* **87**, 1153-1135.

Fong, G. H., Rossant, J., Gertsenstein, M. and Breitman, M. L. (1995). Role of the Flt-1 receptor tyrosine kinase in regulating the assembly of vascular endothelium. *Nature* **376**, 66-70.

Goodrich, L. V., Milenkovic, L., Higgins, K. M. and Scott, M. P. (1997). Altered neural cell fates and medulloblastoma in mouse patched mutants. *Science* **277**, 1109-1113.

Grabel, L., Becker, S., Lock, L., Maye, P. and Zanders, T. (1998). Using EC and ES cell culture to study early development: recent observations on Indian hedgehog and Bmps. *Int. J. Dev. Biol.* **42**, 917-925.

Hammerschmidt, M., Brook, A. and McMahon, A. P. (1997). The world according to hedgehog. *Trends Genet.* **13**, 14-21.

Hirashima, M., Kataoka, H., Nishikawa, S. and Matsuyoshi, N. (1999). Maturation of embryonic stem cells into endothelial cells in an in vitro model of vasculogenesis. *Blood* **93**, 1253-1263.

Hirschi, K. K., Rohovsky, S. A. and D'Amore, P. A. (1998). PDGF, TGF-beta, and heterotypic cell-cell interactions mediate endothelial cell-induced recruitment of 10T1/2 cells and their differentiation to a smooth muscle fate. *J. Cell Biol.* **141**, 805-814.

Huang, Z. F., Higuchi, D., Lasky, N. and Broze, G. J., Jr (1997). Tissue factor pathway inhibitor gene disruption produces intrauterine lethality in mice. *Blood* **90**, 944-951.

Hungerford, J. E. and Little, C. D. (1999). Developmental biology of the vascular smooth muscle cell: building a multilayered vessel wall. *J. Vasc. Res.* **36**, 2-27.

Karp, S. J., Schipani, E., St-Jacques, B., Hunzelman, J., Kronenberg, H. and McMahon, A. P. (2000). Indian hedgehog coordinates endochondral bone growth and morphogenesis via parathyroid hormone related-protein-dependent and independent pathways. *Development* **127**, 543-548.

Kruger, O., Plum, A., Kim, J. S., Winterhager, E., Maxeiner, S., Hallas, G., Kirchhoff, S., Traub, O., Lamers, W. H. and Willecke, K. (2000). Defective vascular development in connexin 45-deficient mice. *Development* **127**, 4179-4193.

Li, D. Y., Sorensen, L. K., Brooke, B. S., Urness, L. D., Davis, E. C., Taylor, D. G., Boak, B. B. and Wendel, D. P. (1999). Defective angiogenesis in mice lacking endoglin. *Science* **284**, 1534-1537.

Maye, P., Becker, S., Kasameyer, E., Byrd, N. and Grabel, L. (2000). Indian hedgehog signaling in extraembryonic endoderm and ectoderm differentiation in ES embryoid bodies. *Mech. Dev.* **94**, 117-132.

McMahon, A. P. (2000). More surprises in the Hedgehog signaling pathway. *Cell* **100**, 185-188.

Mortensen, R. M., Conner, D. A., Chao, S., Geisterfer-Lowrance, A. A. and Seidman, J. G. (1992). Production of homozygous mutant ES cells with a single targeting construct. *Mol. Cell Biol.* **12**, 2391-2395.

Murone, M., Rosenthal, A. and de Sauvage, F. J. (1999). Sonic hedgehog signaling by the patched-smoothened receptor complex. *Curr. Biol.* **9**, 76-84.

Palis, J., McGrath, K. E. and Kingsley, P. D. (1995). Initiation of hematopoiesis and vasculogenesis in murine yolk sac explants. *Blood* **86**, 156-163.

Pepicelli, C. V., Lewis, P. M. and McMahon, A. P. (1998). Sonic hedgehog regulates branching morphogenesis in the mammalian lung. *Curr. Biol.* **8**, 1083-1086.

Pola, R., Ling, L. E., Silver, M., Corbley, M. J., Kearney, M., Blake Pepinsky, R., Shapiro, R., Taylor, F. R., Baker, D. P., Asahara, T. et al. (2001). The morphogen Sonic hedgehog is an indirect angiogenic agent upregulating two families of angiogenic growth factors. *Nat. Med.* **7**, 706-711.

Ramalho-Santos, M., Melton, D. A. and McMahon, A. P. (2000). Hedgehog signals regulate multiple aspects of gastrointestinal development. *Development* **127**, 2763-2772.

Risau, W. (1997). Mechanisms of angiogenesis. *Nature* **386**, 671-674.

Risau, W. and Flamme, I. (1995). Vasculogenesis. *Annu. Rev. Cell Dev. Biol*. **11**, 73-91.

Robb, L. and Elefanty, A. G. (1998). The hemangioblast–an elusive cell captured in culture. *BioEssays* **20**, 611-614.

Robb, L., Lyons, I., Li, R., Hartley, L., Kontgen, F., Harvey, R. P., Metcalf, D. and Begley, C. G. (1995). Absence of yolk sac hematopoiesis from mice with a targeted disruption of the scl gene. *Proc. Natl. Acad. Sci. USA* **92**, 7075-7079.

Rowitch, D. H., St-Jacques, B., Lee, S. M., Flax, J. D., Snyder, E. Y. and McMahon, A. P. (1999). Sonic hedgehog regulates proliferation and inhibits differentiation of CNS precursor cells. *J. Neurosci.* **19**, 8954-8965.

Sato, T. N., Tozawa, Y., Deutsch, U., Wolburg-Buchholz, K., Fujiwara, Y., Gendron-Maguire, M., Gridley, T., Wolburg, H., Risau, W. and Qin, Y. (1995). Distinct roles of the receptor tyrosine kinases Tie-1 and Tie-2 in blood vessel formation. *Nature* **376**, 70-74.

Shalaby, F., Rossant, J., Yamaguchi, T. P., Gertsenstein, M., Wu, X. F., Breitman, M. L. and Schuh, A. C. (1995). Failure of blood-island formation and vasculogenesis in Flk-1-deficient mice. *Nature* **376**, 62-66.

St-Jacques, B., Hammerschmidt, M. and McMahon, A. P. (1999). Indian hedgehog signaling regulates proliferation and differentiation of chondrocytes and is essential for bone formation. *Genes Dev.* **13**, 2072-2086.

Visvader, J. E., Fujiwara, Y. and Orkin, S. H. (1998). Unsuspected role for the T-cell leukemia protein SCL/tal-1 in vascular development. *Genes Dev.* **12**, 473-479.

Vittet, D., Prandini, M. H., Berthier, R., Schweitzer, A., Martin-Sisteron, H., Uzan, G. and Dejana, E. (1996). Embryonic stem cells differentiate in vitro to endothelial cells through successive maturation steps. *Blood* **88**, 3424-3431.

Vittet, D., Buchou, T., Schweitzer, A., Dejana, E. and Huber, P. (1997). Targeted null-mutation in the vascular endothelial-cadherin gene impairs the organization of vascular-like structures in embryoid bodies. *Proc. Natl. Acad. Sci. USA* **94**, 6273-62738.

Wickramasinghe, D., Becker, S., Ernst, M. K., Resnick, J. L., Centanni, J. M., Tessarollo, L., Grabel, L. B. and Donovan, P. J. (1995). Two CDC25 homologues are differentially expressed during mouse development. *Development* **121**, 2047-2056.

Wilkinson, D. G., Bailes, J. A., Champion, J. E. and McMahon, A. P. (1987). A molecular analysis of mouse development from 8 to 10 days post coitum detects changes only in embryonic globin expression. *Development* **99**, 493-500.

Wood, H. B., May, G., Healy, L., Enver, T. and Morriss-Kay, G. M. (1997). CD34 expression patterns during early mouse development are related to modes of blood vessel formation and reveal additional sites of hematopoiesis. *Blood* **90**, 2300-2311.

Zhang, X., Ramalho-Santos, M. and McMahon, A. (2001). *Smoothened* mutants reveal redundant roles for Shh and Ihh Signaling including regulation of L/R asymmetry by the mouse node. *Cell* **105**, 751-792.